



## 3D-QSAR, DOCKING AND PHARMCOPHORE MAPPING OF SUBSTITUTED IMIDAZOLE BASED ANTI-MICROBIAL DERIVATIVES

Shiv Jee Kashyap<sup>1\*</sup>, Narendra Silawat<sup>2</sup>

---

**Article History:**

**Received:** 02/11/22

**Revised:** 17/11/22

**Accepted:** 29/11/22

---

**Abstract:**

Bacterial disease remains one of the most widespread and leading deadliest diseases that result in 1.4 million deaths and 10.4 million clinical cases in the year 2015, and both are in continual increase, especially in developing countries according to the World Health Organization (WHO) 2016 report. Quantitative structure-activity and relationships, often simply known as QSAR, is an analytical application that can be used to interpret the quantitative relationship between the biological activities of a particular molecule and its structure. Imidazole are one of the most important classes of nitrogen containing heterocycles that exhibited various biological activities. Based on the SAR study generated by molecular modelling analysis, one hundred and ten novel oxidoreductase inhibitor derivatives were successfully designed exhibiting moderate predicted activities in all three applied computational approaches. The binding mode of the imidazole analogues was clarified by the flexible docking method and Hydrogen bonding interaction and hydrophobic interaction were found to be important for the imidazole analogues binding on PDB.

**Keywords:** Imidazole, oxidoreductase inhibitor, Docking, Pharmacophore, molecular modelling.

---

<sup>1\*</sup>Research Scholar, Faculty of Pharmacy, Oriental University, Indore-India, Email: shivjee10@gmail.com

<sup>2</sup>Professor, Faculty of Pharmacy, Oriental University, Indore-India

**\*Corresponding Author:** Shiv Jee Kashyap

\*Research Scholar, Faculty of Pharmacy, Oriental University, Indore-India, Email: shivjee10@gmail.com

**DOI:** 10.53555/ecb/2022.11.12.191

## INTRODUCTION:

Infectious diseases raise awareness of our global vulnerability, the need for strong health care systems and the potentially broad and borderless impact of disease. The human body exists in a state of dynamic equilibrium with microorganism. In a healthy individual this balance is maintained as peaceful co-existence and lack of disease [1]. But sometimes, micro-organisms cause an infection or a disease.

The main objective of QSAR is to observe the biological responses of a set of molecules, measure it, and statistically relate the measured activity to some molecular structure on their surface. The product of QSAR will then produce useful equations, images or models in either 2D or 3D form that would relate their biological responses or physical properties to their molecular structure. Quantitative structure-activity and relationships, often simply known as QSAR, is an analytical application that can be used to interpret the quantitative relationship between the biological activities of a particular molecule and its structure. It is considered a major method of chemical researching all over the world today and is frequently used in agricultural, biological, environmental, medicinal, and physical organic studies. [2].

The three dimensional structures known may be represented to show different views of the structures. With complex molecular mechanics programs it is possible to superimpose one structure on another. The same approach is used to superimpose the three dimensional structure of a potential drug on its possible target site. This process, which is often automated, is known as docking. Molecular docking is used to predict the structure of the intermolecular complex formed between two molecules. The small molecule called Ligand usually interacts with protein's binding sites. Binding sites are areas of protein known to be

active in forming of compounds. There are several possible mutual conformations in which binding may occur. These are commonly called binding modes [4].

It also predicts the strength of the binding, the energy of the complex; the types of signal produced and calculate the binding affinity between two molecules using scoring functions. The most interesting case is the type protein-ligand interaction, which has its applications in medicine. Imidazole is an organic compound with the formula  $C_3N_2H_4$ . It is a white or colourless solid that is soluble in water, producing a mildly alkaline solution. In chemistry, it is an aromatic heterocycle, classified as a diazole, and has non-adjacent nitrogen atoms in meta-substitution[3].

Many natural products, especially alkaloids, contain the imidazole ring. These imidazoles share the 1,3- $C_3N_2$  ring but feature varied substituents. This ring system is present in important biological building blocks, such as histidine [5] and the related hormone histamine. Many drugs contain an imidazole ring, such as certain antifungal drugs, the nitroimidazole series of antibiotics, and the sedative midazolam

## EXPERIMENTAL WORK:

### Selection and Description of PDB:

The protein structure of pdb name along with their inhibitors was retrieved from RCSB Protein Data Bank (PDB entry code: 5JFO).

**PDB:** 5JFO (M.tuberculosis enoyl-reductaseInhA in complex with GSK625) [6].

Name of Ligand: ACR

Chemical name of the ligand: N-{1-[(2-chloro-6-fluorophenyl)methyl]-1H-pyrazol-3-yl}-5-[(1S)-1-(3-methyl-1H-pyrazol-1-yl)ethyl]-1,3,4-thiadiazol-2-amine

Chemical Formula :  $C_{21}H_{27}N_7O_{14}P_2$

Structure Ligand:

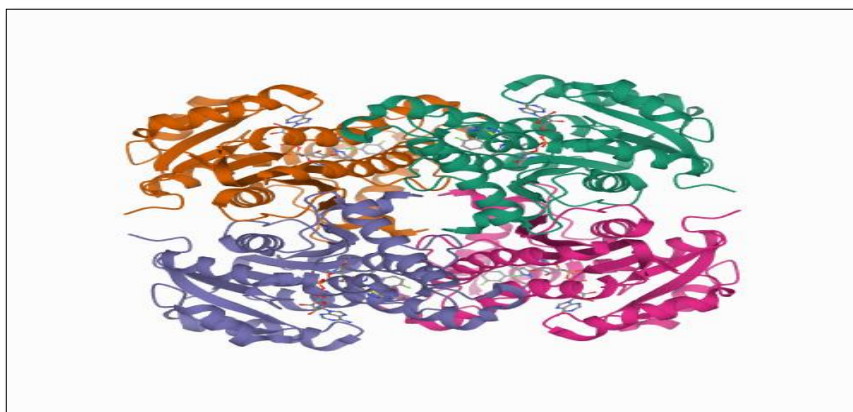
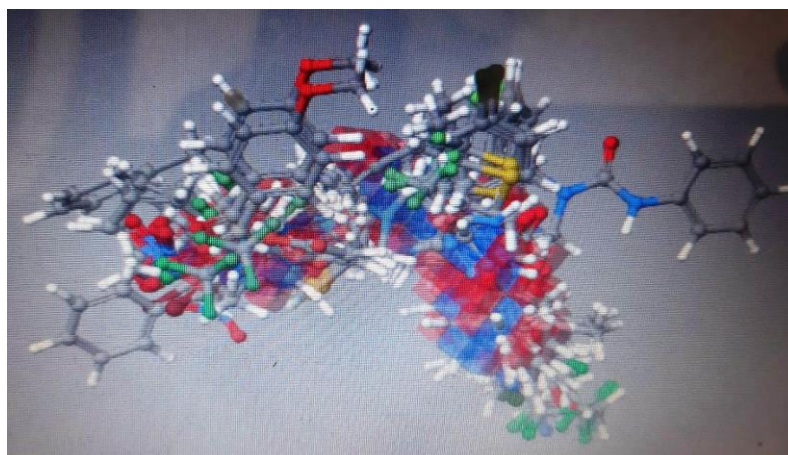


Figure 1: 3D view of PDB 5JFO

### STRUCTURAL ALIGNMENT:

The molecular modelling studies were performed using SYBYL X2.0 software (Tripos) running on a core-2 duo Intel processor workstation [7]. The

molecules to be analysed were aligned on an appropriate template, which is considered to be common substructure.



**Figure 2: Alignment of all selected molecules**

### 3D-QSAR STUDIES:

#### CoMFA

The aligned sets of molecules were positioned inside four grids boxes with grid spacing values of 1.5, 2.0, 2.5 and 3.0 Å in all Cartesian directions and CoMFA fields were calculated using the QSAR modules of SYBYL. The interaction energies for each molecule were calculated at each grid point using two probe atoms: an  $sp^3$  hybridised carbon atom with van der Waals radius of 1.52 Å and a +1.0 charge (default probe) and an  $sp^3$  hybridised oxygen atom with a vdW radius of 1.38 Å and a -1.0 charge.

#### CoMSIA

CoMSIA similarity index descriptors were derived using the same lattice boxes as those used in CoMFA calculations. Five properties, i.e., steric (S), electrostatic (E), hydrophobic (H), hydrogen bond donor (D) and hydrogen bond acceptor (A), were evaluated using a probe atom of 1.0 Å radius and +1.0 charge. In CoMSIA, the steric indices are related to the third power of the atomic radii, the electrostatic descriptors are derived from atomic partial charges, the hydrophobic fields are derived from atom – based parameters developed by Vishwanath and co-workers, and the hydrogen bond donor and acceptor indices are obtained from a rule-based method derived from experimental values [8].

#### HQSAR

HQSAR is a new 2D-QSAR technique which employs specialized fragment fingerprints as predictive variables of biological activity. HQSAR does not require 3D alignment for model

generation and is sensitive to three parameters concerning hologram generation, including hologram length, fragment size, and fragment distinction. The fragment distinct are atoms (A), bonds (B), connections (C), hydrogen atom (H), chirality (Ch), and donor (D) [8, 9]. Initially, various models were developed by using the default fragment size of 4-7 and different component, then based on the different fragment distinction determined by the first step, the models were developed using different sizes.

### DOCKING ANALYSIS

Molecular docking studies were carried out using the Schrödinger Maestro version 2016. The protein structure of pdb name along with their inhibitors was retrieved from RCSB Protein Data Bank (PDB entry code: 5JFO) [7]. The protein structures were subjected to energy minimization and charge calculation (MMFF94). After that the known complex protein structure was used to investigate and validate the docking protocol. All ligand and water molecules were removed [10]. The bloat values was set as 1 and the threshold values as 0.5 for generation of protomol and position was considered to be the active sites for potential receptor's binding sites.

### PHARMACOPHORE MAPPING:

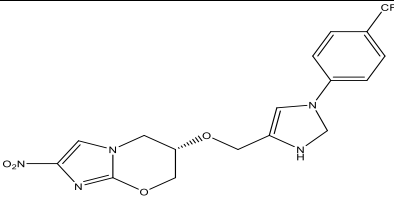
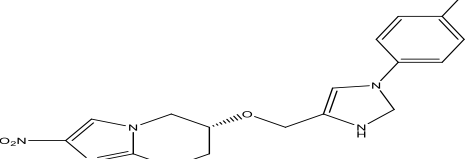
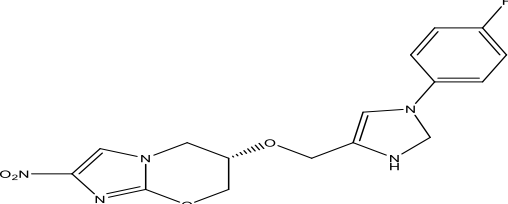
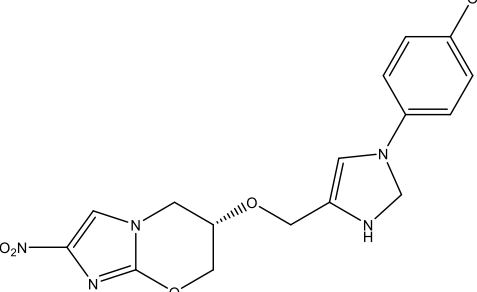
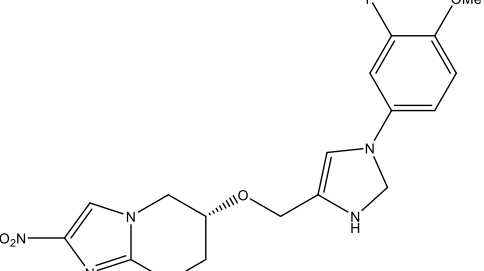
Genetic algorithm with linear assignment of hypermolecular alignment of datasets (GALAHAD) was used to generate the pharmacophore models. All the s in the training set were prepared by the following procedures; the structures were checked for bond orders, hydrogen

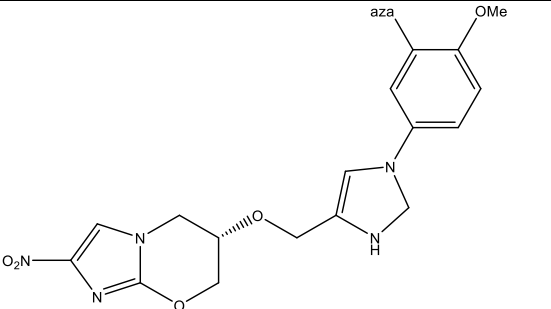
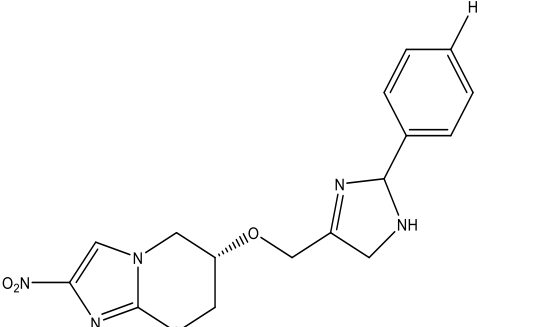
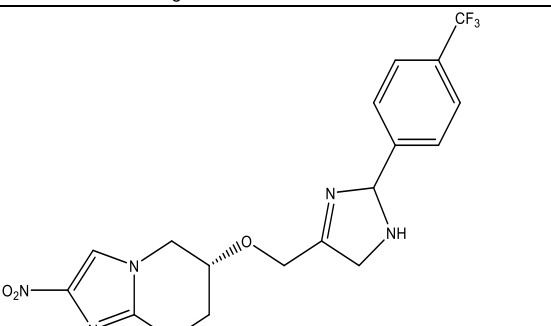
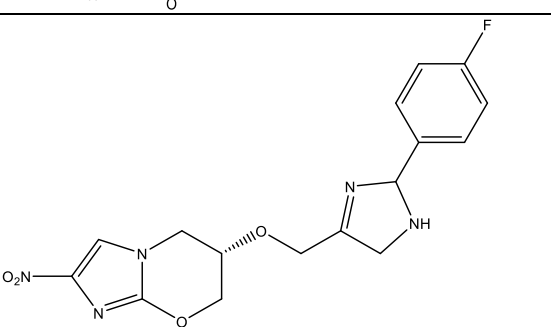
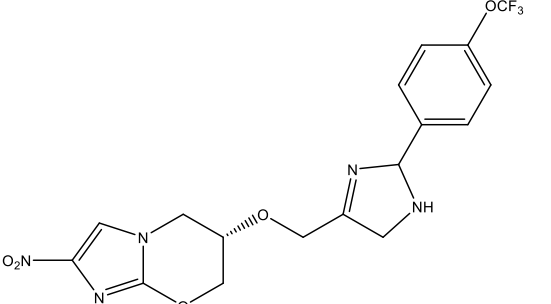
atoms were added and minimization procedures was implemented using the MMFF94, force-field GALAHAD was run for 60 generation with a population size of 100. The rest of the parameters were set as default values [11,12]. The generated models were evaluated by a test database; several parameters were employed for model evaluation.

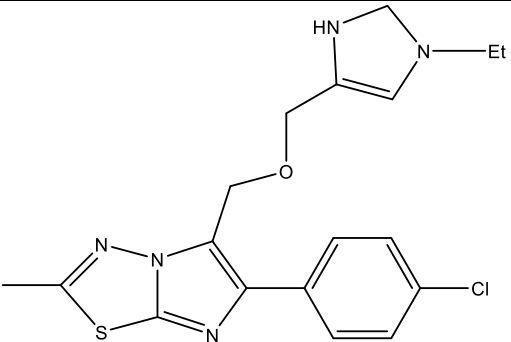
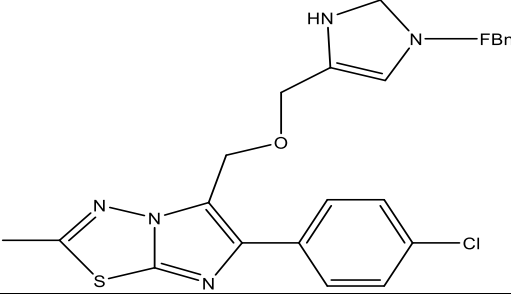
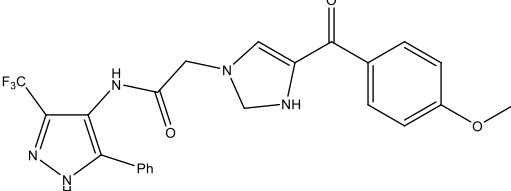
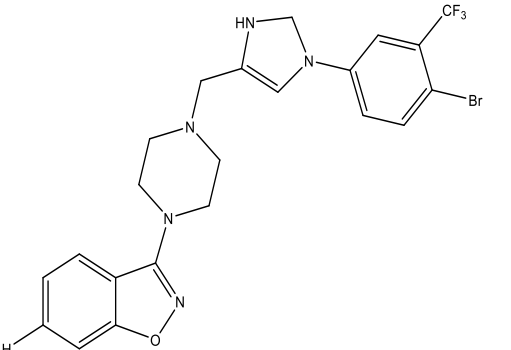
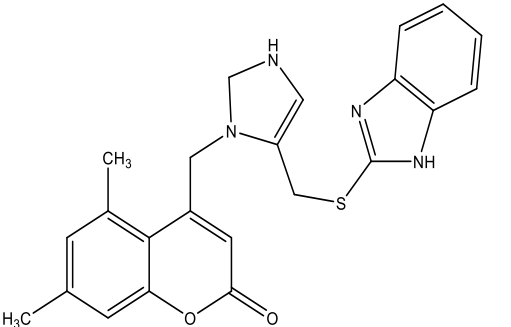
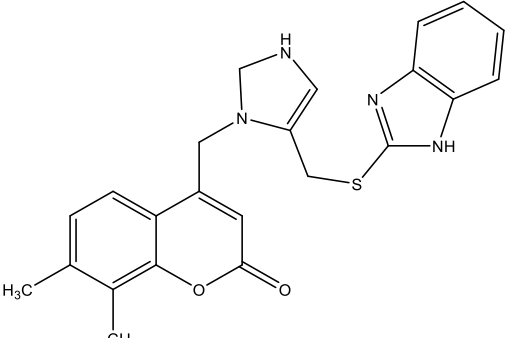
### DESIGNING OF COMPOUNDS:

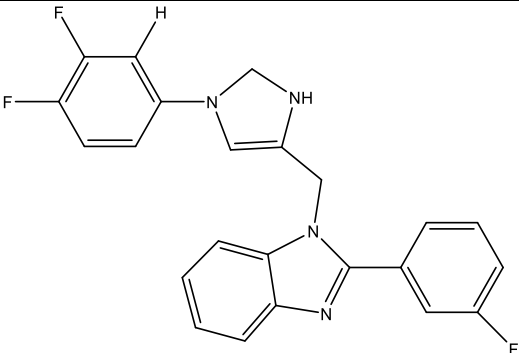
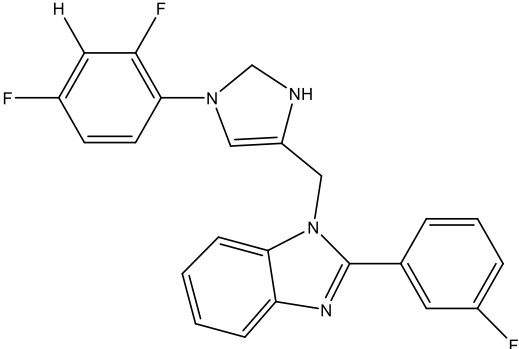
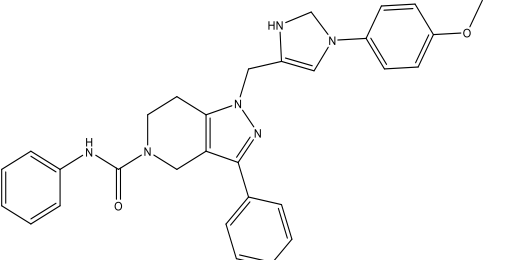
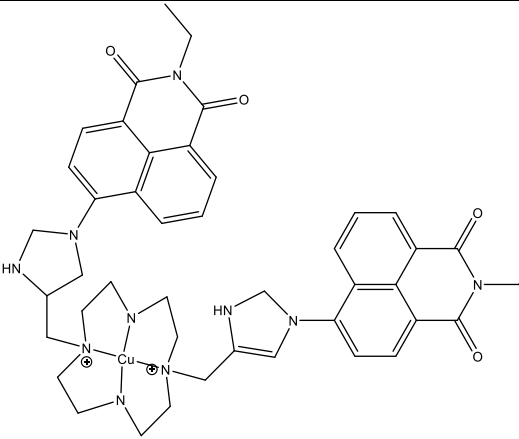
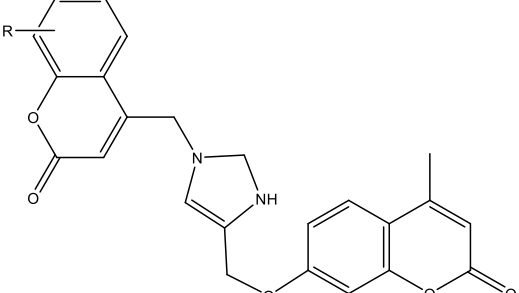
On the basis of reported structure activity relationship of imidazole analogues as an  $\alpha$  - oxidosidase inhibitor ,QSAR studies using CoMFA, CoMSIA, HQSAR, and Molecular modelling (Docking ) studies , one hundred and two compounds were designed [13-15]. On the designed compounds, further Computational QSAR studies CoMFA, CoMSIA, HQSAR and Molecular modelling Docking was done in order to select the best compounds for synthesis.

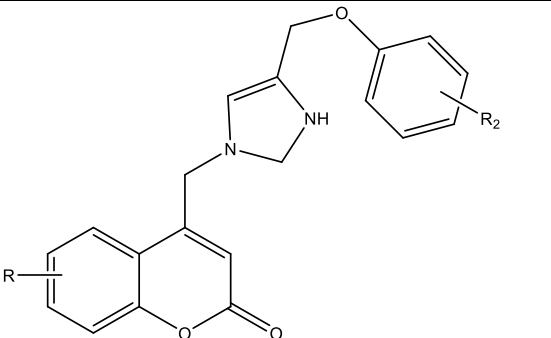
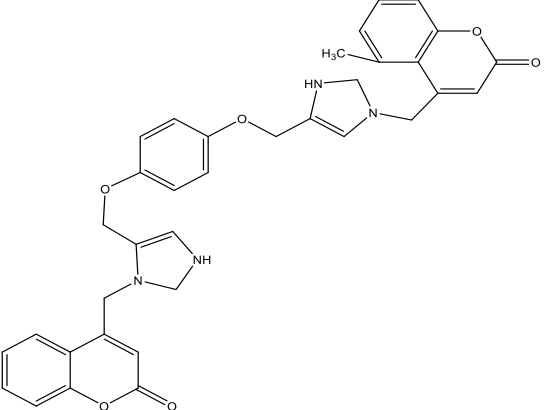
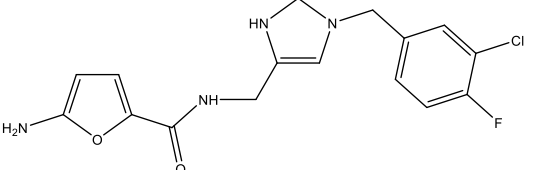
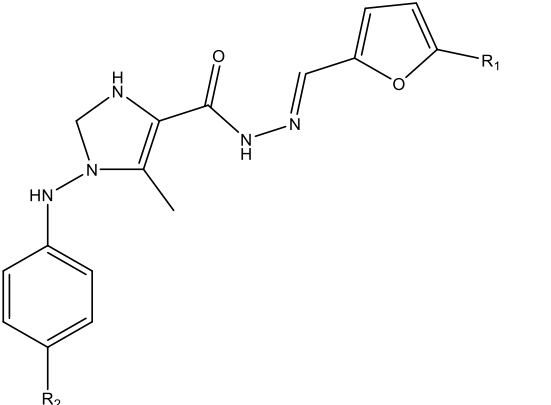
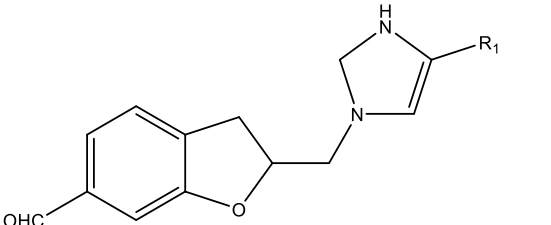
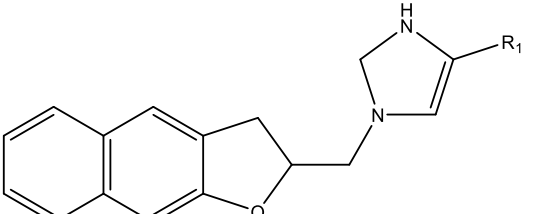
**Table 1:** Designed imidazole analogues on the basis of computational studies with their predicted data:

Compo und	Compound structure	Pred pIC <sub>50</sub>			
		CoMFA	CoMSIA	HQSAR	Docking Score
1	 (S)-2-nitro-6-((1-(4-(trifluoromethyl)phenyl)-2,3-dihydro-1H-imidazol-4-yl)methoxy)-6,7-dihydro-5H-imidazo[2,1-b][1,3]oxazine	4.3521	4.4758	4.282	4.5033
2		4.3484	4.4751	5.03	3.8241
3		4.3438	4.4782	4.328	3.6918
4		4.3534	4.4803	3.836	5.3139
5		4.3477	4.4731	4.696	5.4296

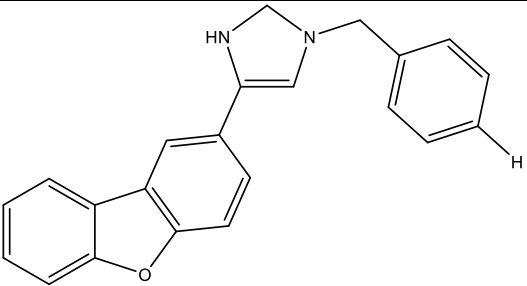
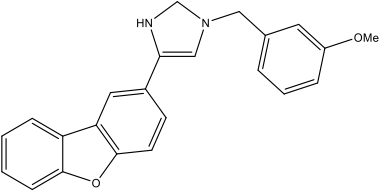
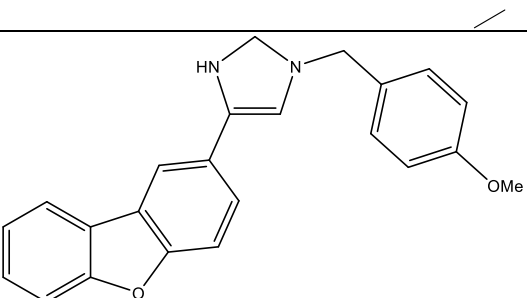
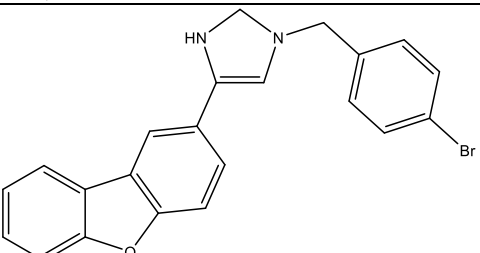
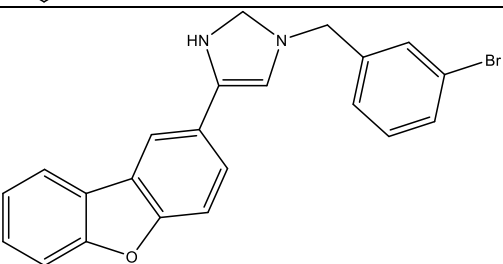
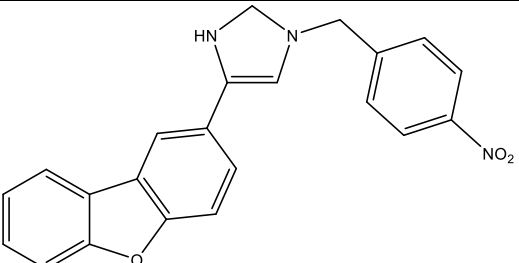
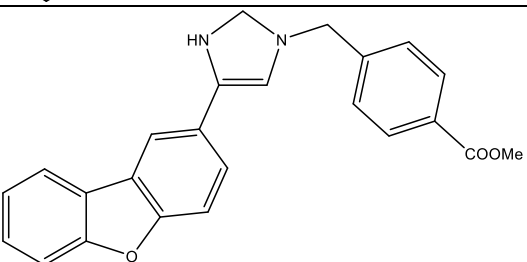
6		4.3456	4.4747	4.915	3.0611
7		4.3488	4.4753	4.578	4.3919
8		4.3493	4.4782	4.447	4.9245
9		4.3486	4.4808	4.425	2.9629
10		4.3502	4.4784	4.756	3.8114

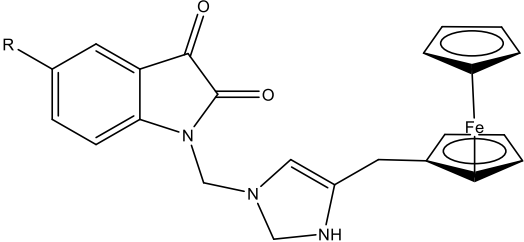
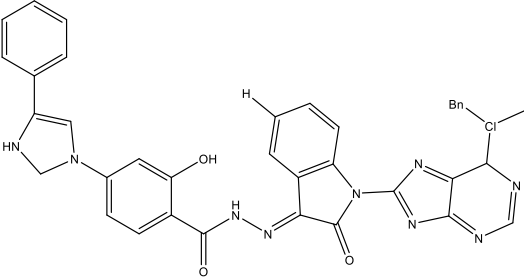
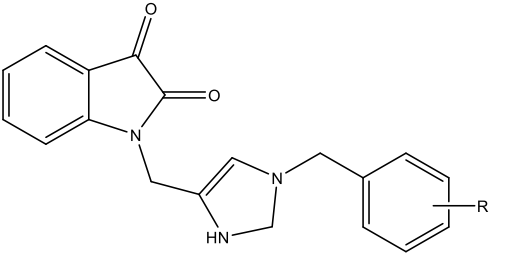
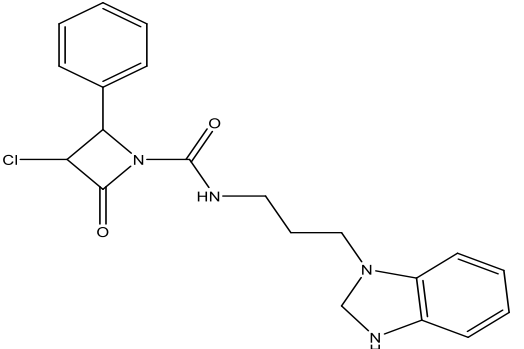
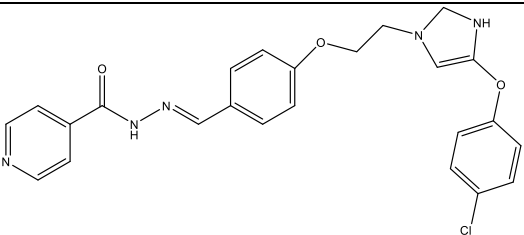
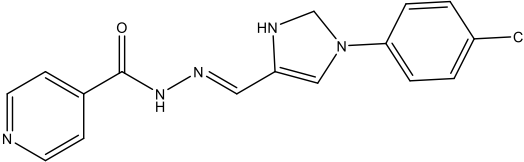
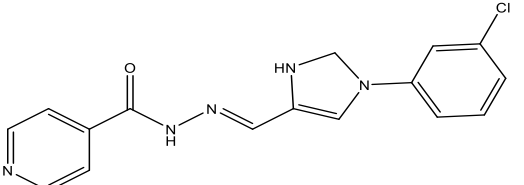
11		4.3511	4.4776	4.503	2.3645
12		4.3450	4.4755	4.518	5.3367
13		4.3493	4.4778	4.341	5.9438
14		4.3443	4.4748	4.594	4.8035
15		4.3536	4.4984	5.123	6.0693
16		4.3456	4.4717	4.597	2.7969

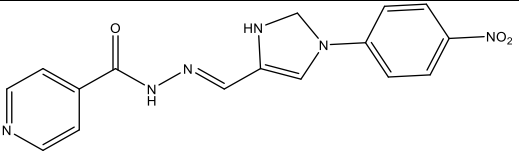
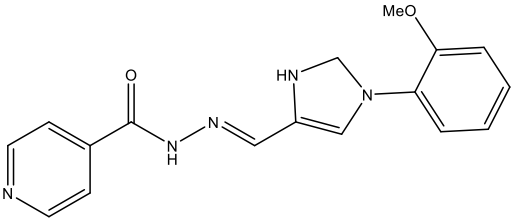
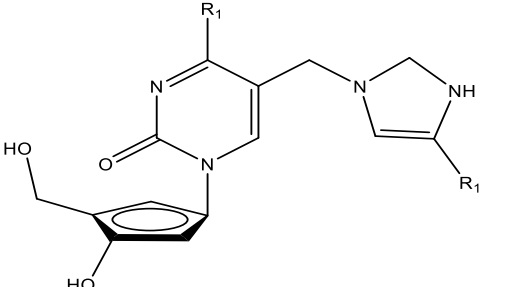
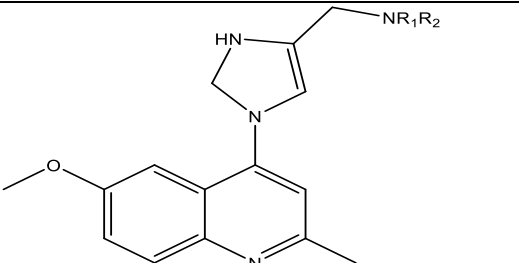
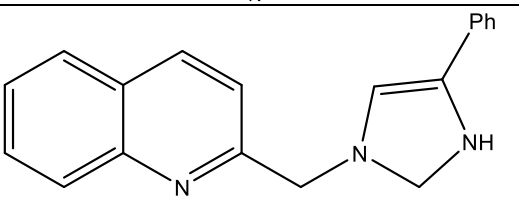
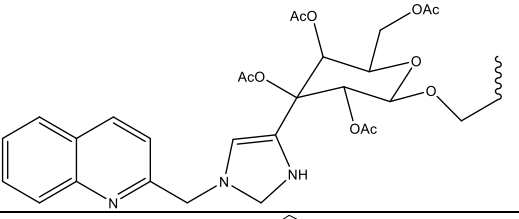
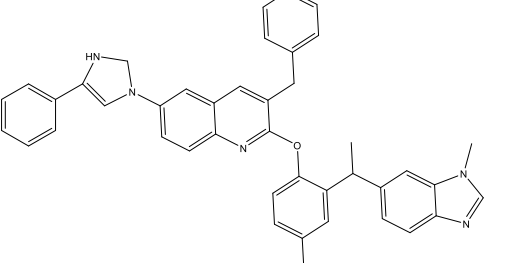
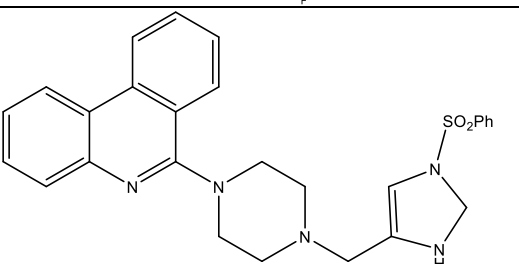
17		4.3462	4.4732	4.725	4.5086
18		4.3469	4.4785	4.691	4.7630
19		4.3495	4.4753	4.823	3.3900
20		4.3480	4.4792	4.941	3.0896
21		4.3461	4.4752	4.647	2.8599

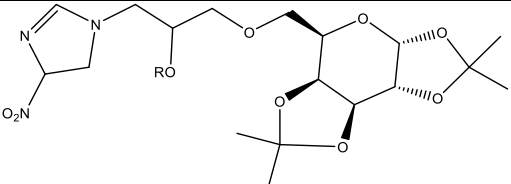
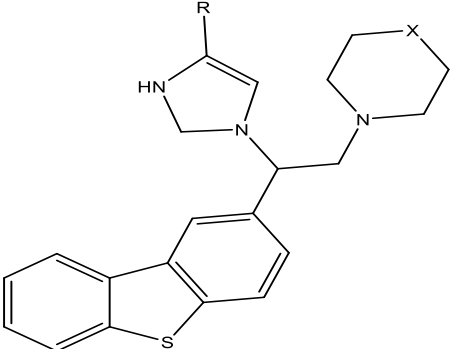
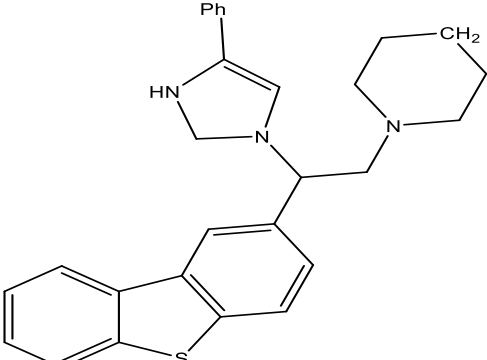
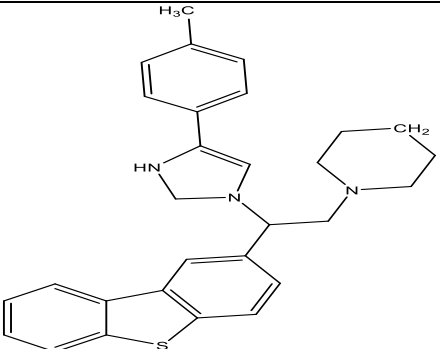
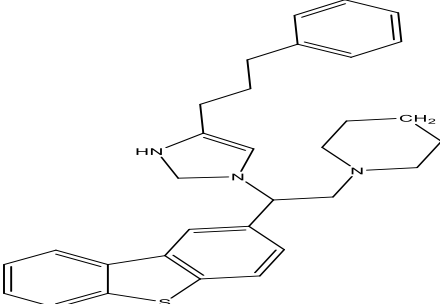
22		4.3492	4.4802	4.518	4.9646
23		4.3465	4.4702	4.866	6.6412
24		4.3452	4.4737	4.826	4.7953
25		4.3467	4.4783	4.742	5.2871
26		4.3453	4.4697	4.884	6.3892
27		4.3514	4.791	4.373	8.2615

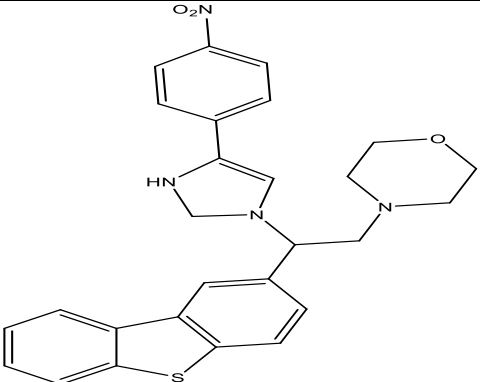
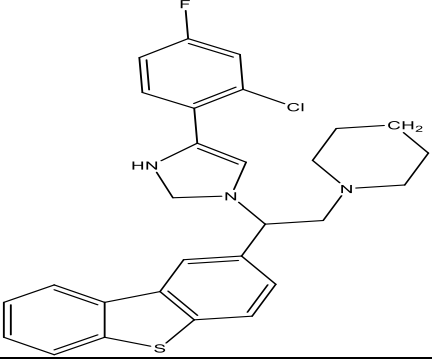
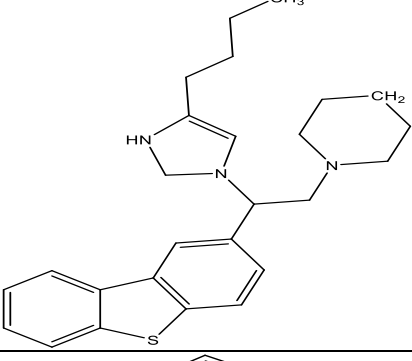
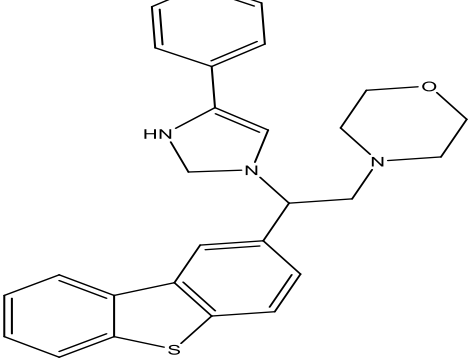
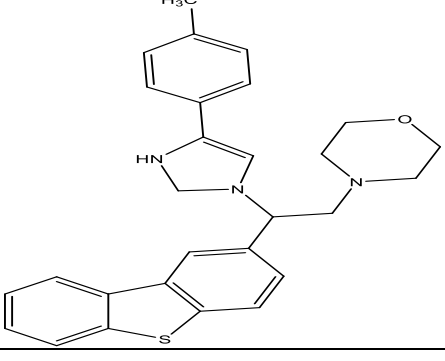


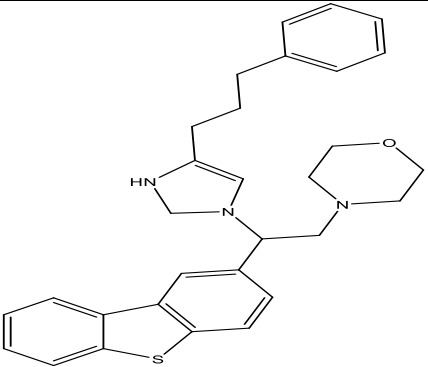
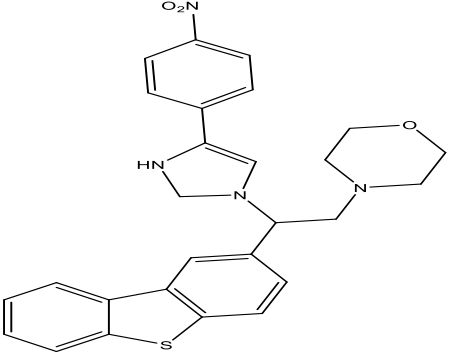
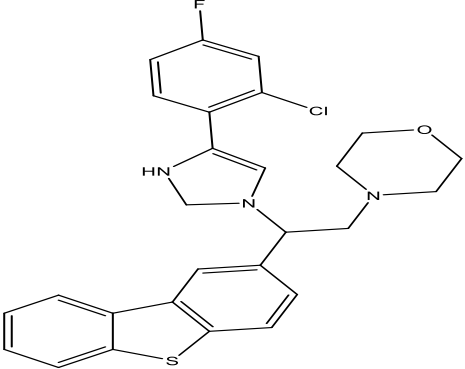
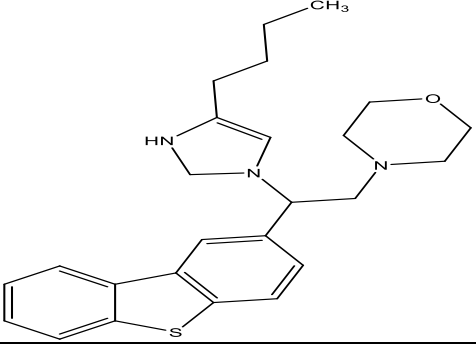
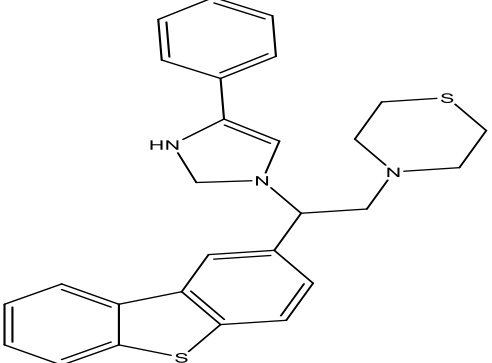
28		4.3473	4.4783	4.293	5.4088
29		4.3470	4.4761	4.939	6.3040
30		4.3431	4.4754	4.775	4.8325
31		4.3454	4.4758	4.555	4.9260
32		4.3501	4.4743	4.859	6.5207
33		4.3520	4.4804	4.182	2.8665
34		4.3474	4.4771	4.624	1.5708

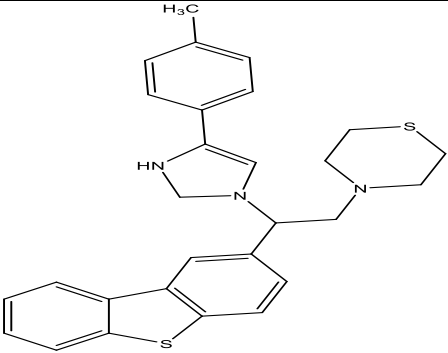
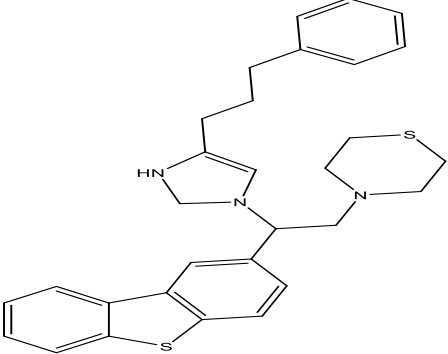
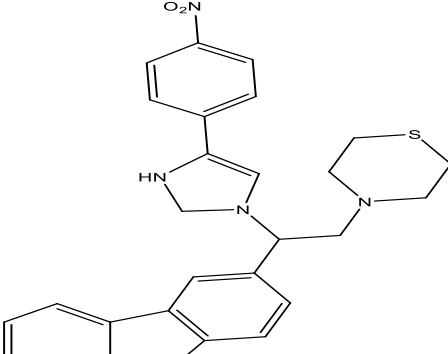
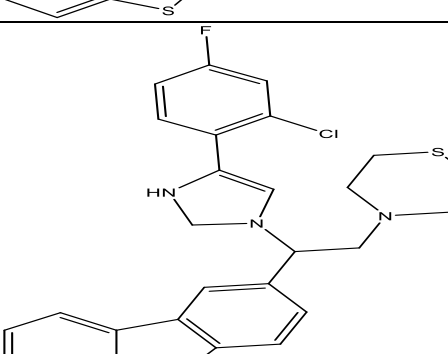
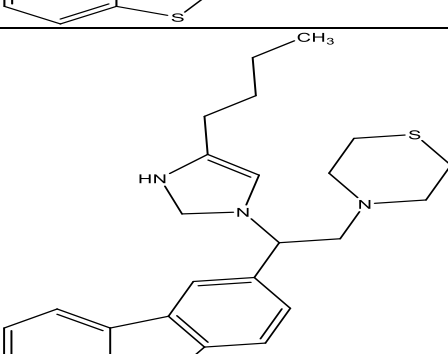
35		4.3503	4.4781	4.378	5.4090
36		4.3459	4.4740	4.876	5.8507
37	 R=CH <sub>3</sub>	4.3541	4.4793	4.745	2.9364
38		4.3471	4.4747	4.796	6.6970
39		4.3451	4.4759	5.016	3.3043
40		4.3460	4.4796	4.654	3.7888
41		4.3508	4.4800	4.947	5.4434

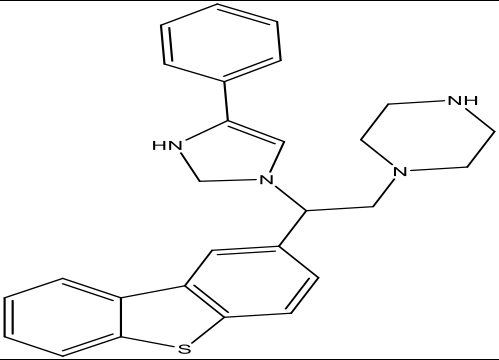
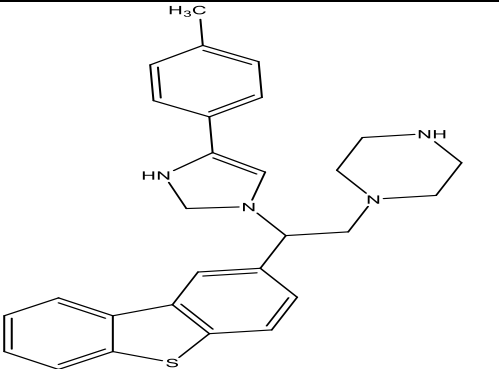
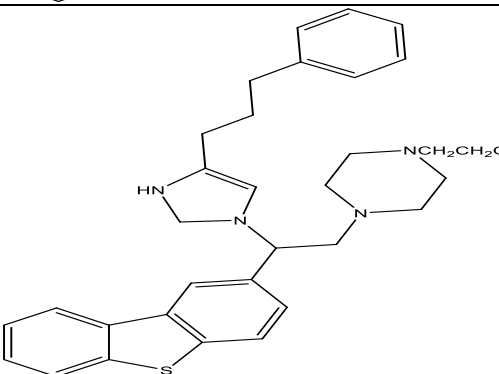
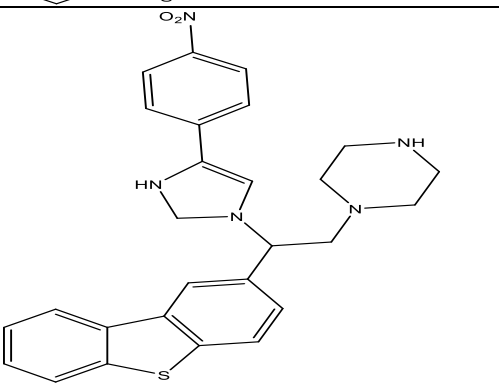
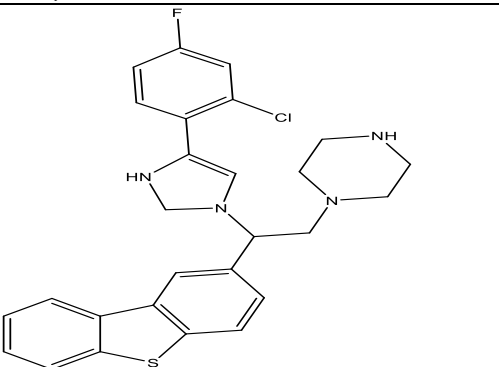
42		4.3467	4.4778	4.883	5.0204
43		4.3460	4.4735	4.876	2.9344
44		4.3436	4.4780	4.596	5.1306
45		4.3466	4.4739	4.721	7.1182
46		4.3453	4.4722	4.774	5.8317
47		4.3496	4.4784	4.341	4.7399
48		4.3457	4.4786	4.138	6.8212
49		4.3492	4.4780	4.884	8.3985

50		4.3506	4.4769	4.617	8.8636
51		4.3534	4.4794	4.872	5.3914
52		4.3452	4.4825	4.118	4.6358
53		4.3407	4.4767	4.721	4.1250
54		4.3337	4.4715	4.019	4.3931

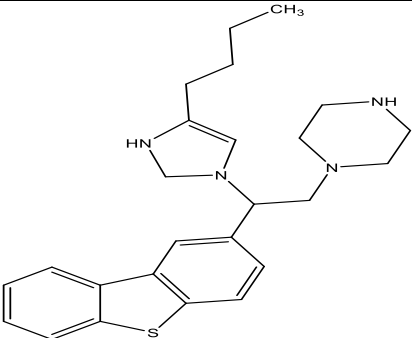
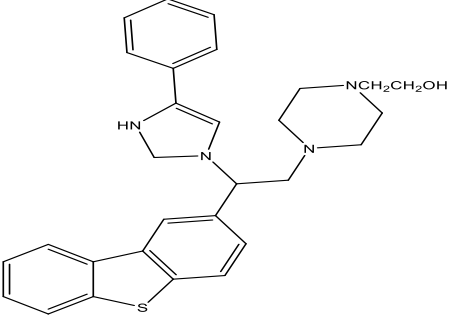
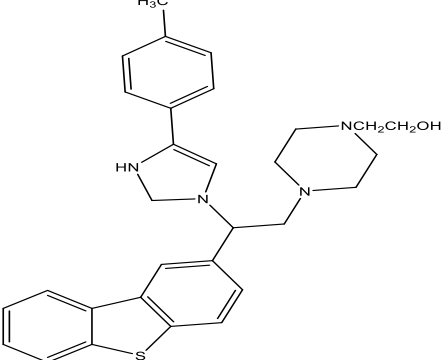
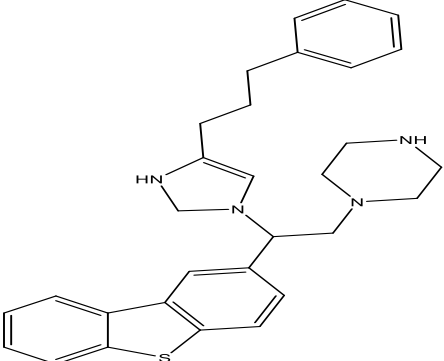
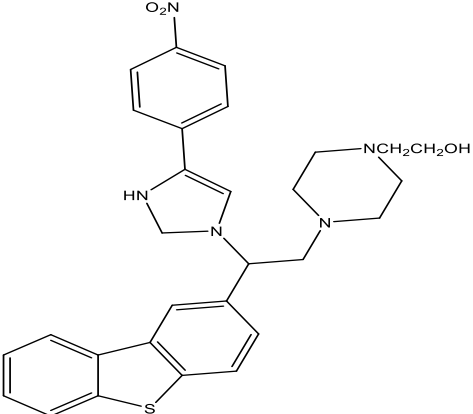
55		4.3493	4.4810	3.527	4.3762
56		4.3333	4.4741	4.387	3.6550
57		4.3369	4.4748	4.606	3.5770
58		4.3357	4.4788	4.269	4.6806
59		4.3387	4.4799	4.137	5.0128

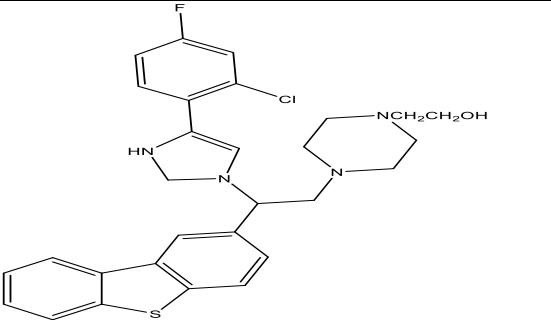
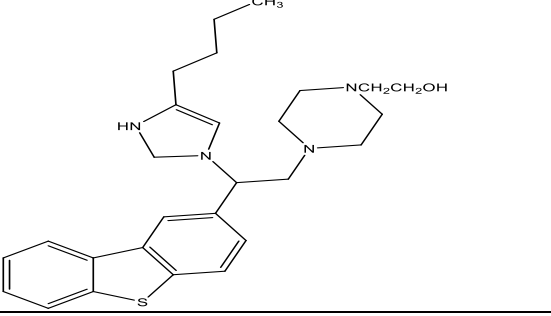
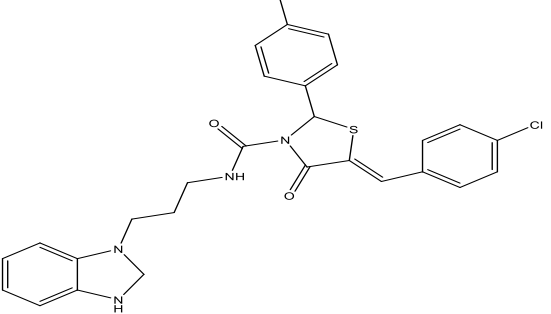
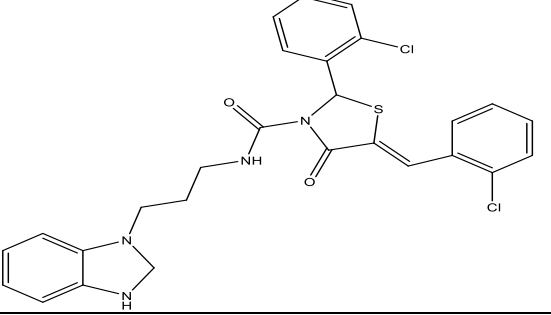
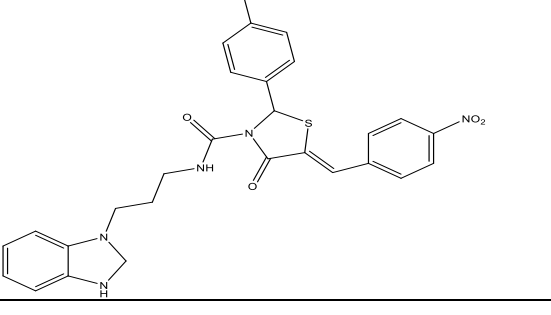
60		4.3391	4.4841	4.116	3.0643
61		4.3340	4.4757	4.447	3.5384
62		4.3432	4.4760	4.193	4.3641
63		4.3346	4.4790	4.208	6.7577
64		4.3416	4.4826	4.032	7.5076

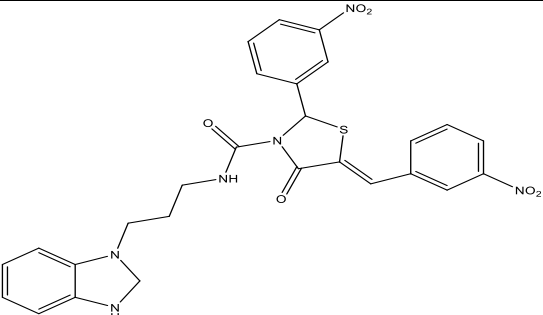
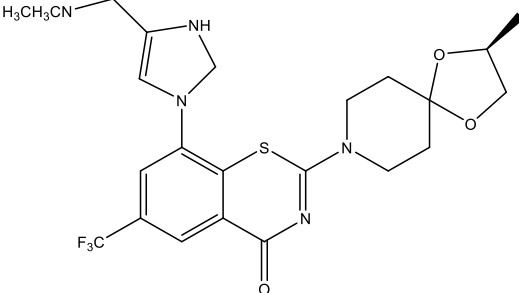
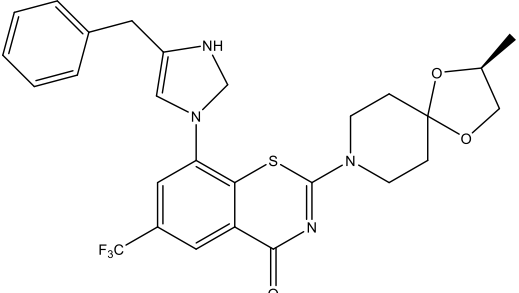
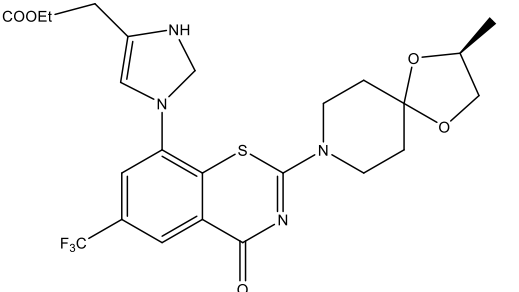
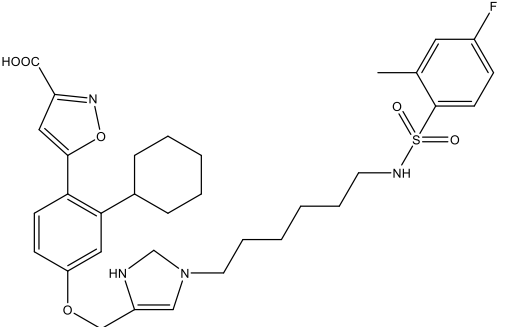
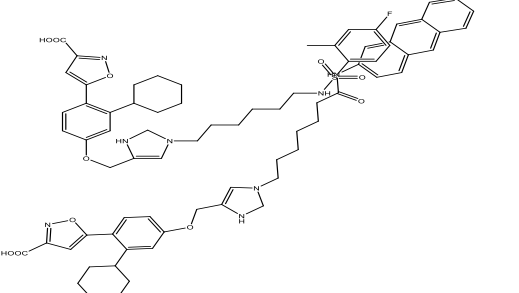
65		4.3332	4.4758	4.285	4.7628
66		4.3472	4.5061	4.814	6.6691
67		4.3332	4.4738	4.288	3.4100
68		4.3387	4.4736	4.415	4.0352
69		4.3325	4.4794	4.382	4.4156

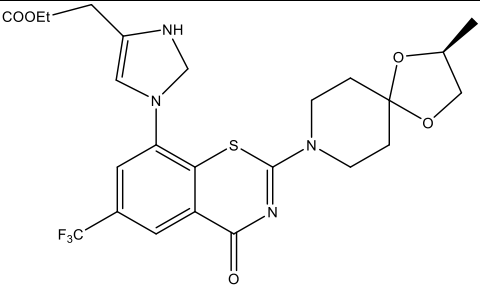
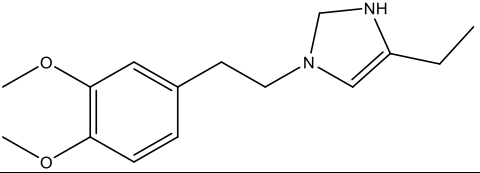
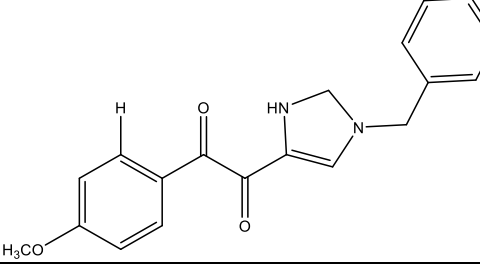
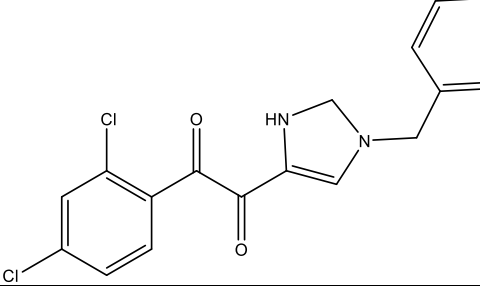
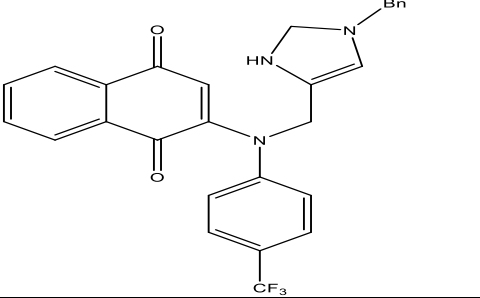
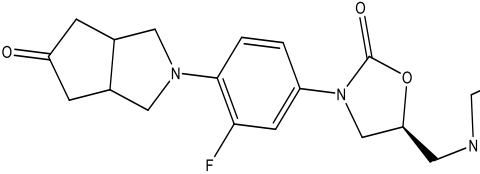
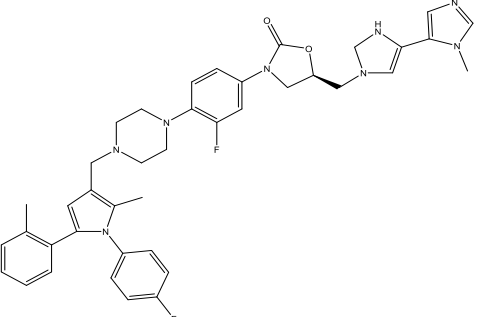
70		4.3435	4.4735	4.514	3.2028
71		4.3430	4.4741	4.631	2.4690
72		4.3355	4.4757	4.338	4.2828
73		4.3354	4.4790	4.208	5.7021
74		4.3320	4.4763	4.556	5.7749



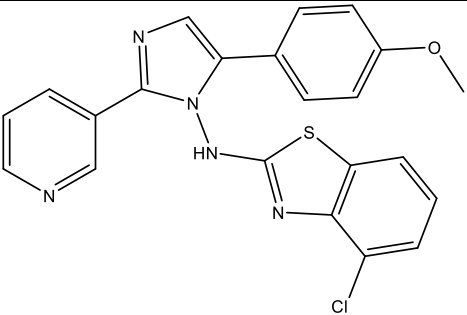
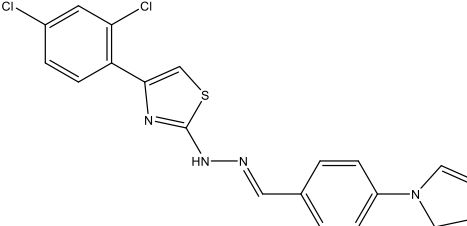
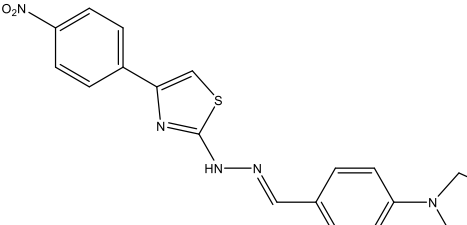
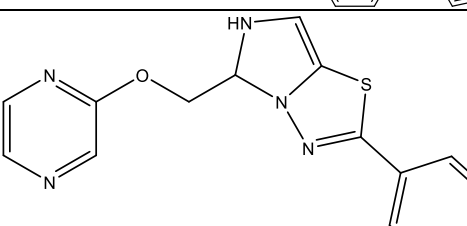
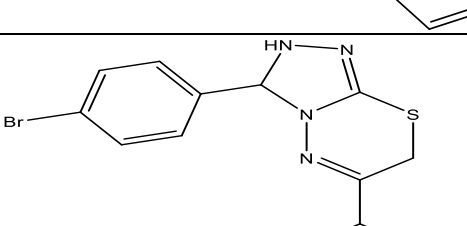
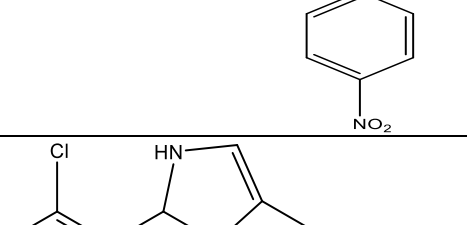
75		4.3352	4.4732	4.517	5.6609
76		4.3348	4.4773	4.433	4.9471
77		4.3306	4.4757	4.575	4.3661
78		4.3350	4.4759	4.428	6.7494
79		4.3378	4.4788	3.984	7.9638

80		4.3361	4.4719	4.629	7.1254
81		4.3276	4.4733	4.466	8.7375
82		4.3353	4.4772	4.246	7.0280
83		4.3350	4.4776	4.55	6.0740
84		4.3416	4.4835	3.873	4.5000

85		4.3405	4.4790	4.315	3.5902
86	<chem>H3C3CN</chem> 	4.3422	4.4739	4.069	5.7215
87		4.3419	4.4705	4.567	5.3869
88	<chem>COOEt</chem> 	4.3496	4.4736	4.436	3.5564
89		4.3365	4.4738	4.487	4.6473
90		4.3331	4.4768	4.707	4.2689

91		4.3382	4.4187	4.467	2.5494
92		4.3362	4.4771	4.638	6.4184
93		4.3367	4.4758	4.574	5.6047
94		4.3361	4.4733	4.567	5.1769
95		4.3407	4.4840	4.287	3.3925
96		4.3322	4.4787	4.412	6.3533
97		4.3330	4.4742	4.465	4.6248

98		4.3389	4.4815	4.032	6.7279
99		4.3357	4.4810	3.828	5.6288
100		4.3427	4.4730	4.575	6.8900
101		4.3413	4.4776	4.308	7.0763
102		4.3509	4.4830	4.563	3.4315
103		4.5241	4.1082	4.465	3.5404
104		4.3542	4.4651	4.638	6.6284

105		4.6365	4.4742	4.542	5.6307
106		4.3382	4.4187	4.467	2.5444
107		4.6262	4.4701	4.645	6.4544
108		4.5477	4.4958	4.530	5.5230
109		4.5651	4.4745	4.677	5.1745
110		4.3580	4.4654	4.547	2.5365

**RESULTS AND DISCUSSION:****CoMFA and CoMSIA Results:**

The results of CoMFA analysis with combination of steric and electrostatic on different charge are summarized. The statistical parameters

corresponding to the CoMFA model are listed. The CoMFA models MMFF94 were generated from training set of 37 molecules with pIC50 value ranging from 3.4661 to 5.2749 using leave-one-out PLS analysis with an optimized component of 1 to

give a good cross-validated correlation coefficient  $q^2$  of 0.787, which suggest that the model should be reasonable tool for predicting the  $IC_{50}$  values. A high non-cross-validated correlation coefficient  $r^2$

of 0.819 with a low standard error estimation (SEE) of 0.041 was obtained as well as an F value of 1316.074 and predictive correlation coefficient  $r^2_{pred}$  of 0.996.

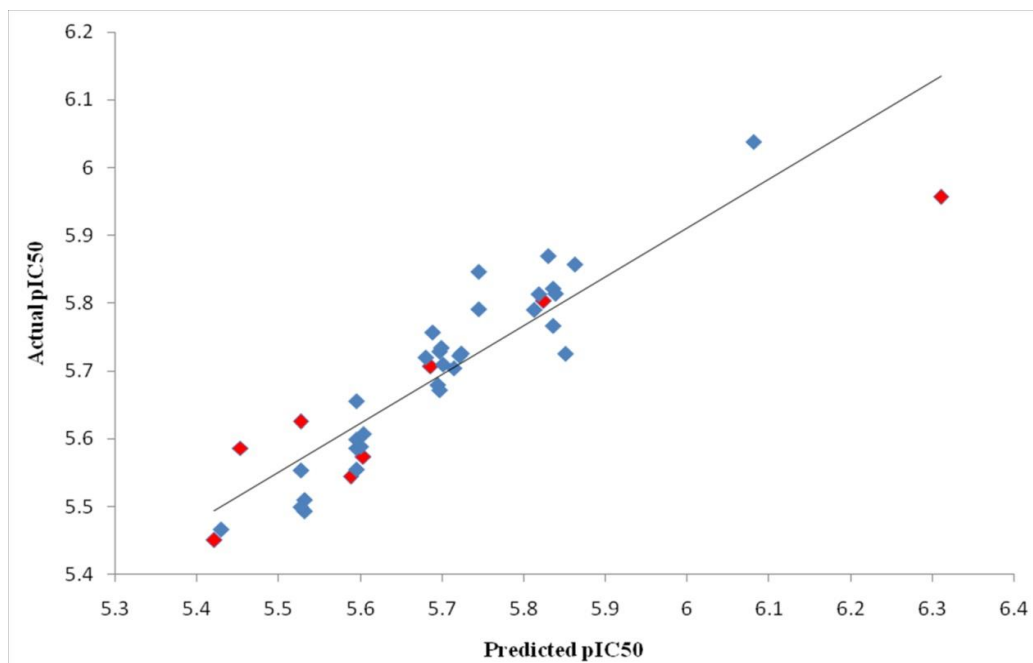


**Figure 3:** Graph of actual versus predicted  $pIC_{50}$  values of the training set and the test set molecules of Model 7 (MMFF94) using the CoMFA model.

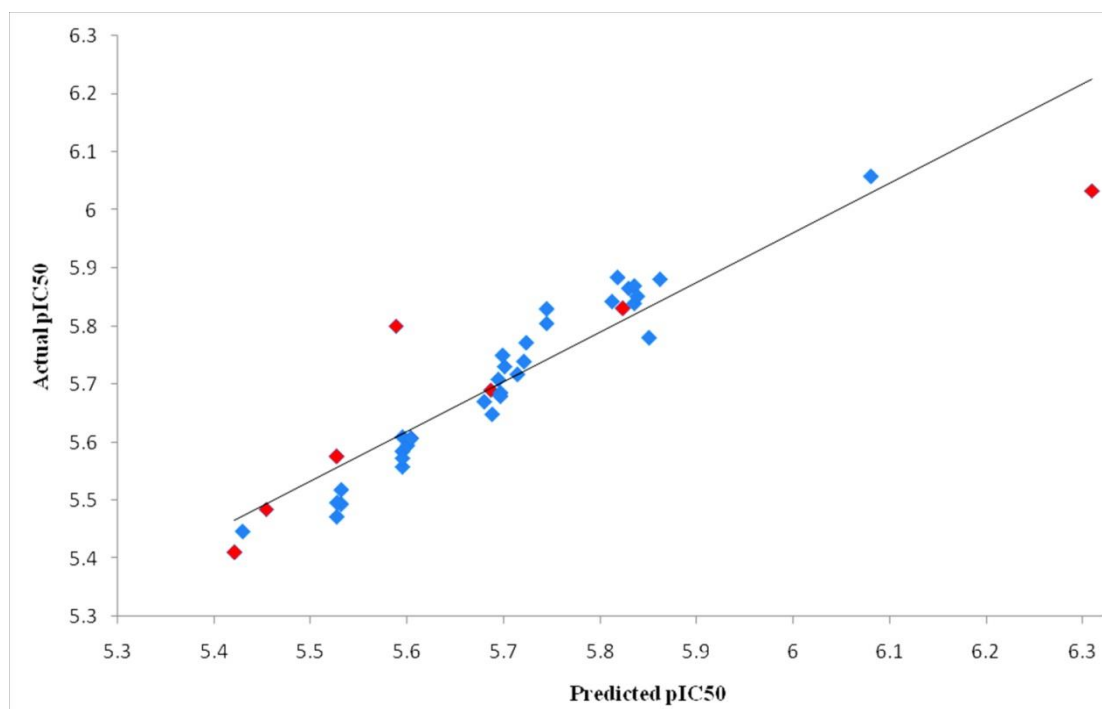


**Figure 4:** Graph of actual versus predicted  $pIC_{50}$  values of the training set and the test set molecules of Model 29 (MMFF94) using the CoMSIA model.

#### H-QSAR Results:

Hologram QSAR modes were developed for a series of 46 compounds (37 training and 9 test). The HQSAR model of training set exhibits significant

*Eur. Chem. Bull.* **2022**, 11(Regular Issue 12), 2358-2384

cross-validated correlation coefficient ( $q^2 = 0.800$ ) and non-cross-validated correlation coefficient ( $r^2 = 0.943$ ). The models were used to predict the inhibitory potencies of the test set compounds and

difference between predicted and experimental values were verified, exhibiting powerful predictive capabilities [16].

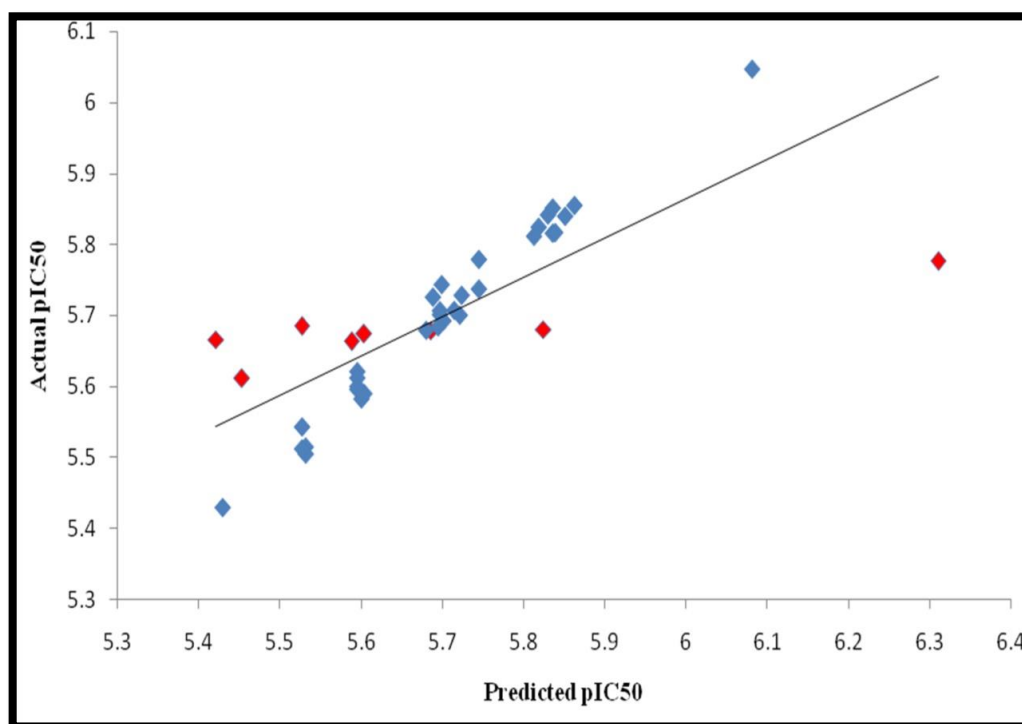


**Figure 5:** Graph of actual versus predicted pIC50 values of the training set and the test set molecules of Model A/B/C at 2-6 fragment size using the HQSAR.

#### Pharmacophore Modelling Results:

Ten GALAHAD models were generated by using training set compounds. Model 8 and 10 had high energy which is considered to be due to steric clashes, leading to their exclusion from the analysis. The other 20 models were generated and

evaluated successively by the test database constructed previously. Table 2 shows the predictable results for each model. Model 8 with the highest value was considered to be the best model.

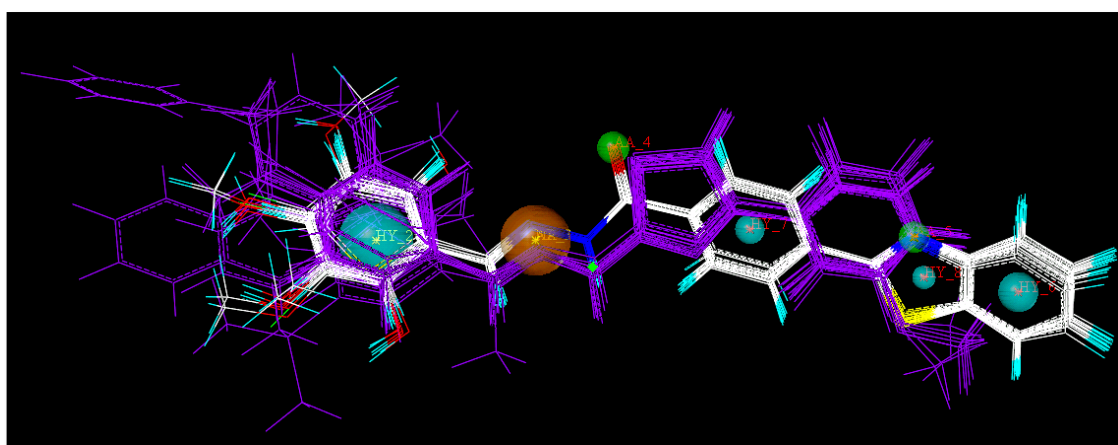


**Figure 6:** Pharmacophore model 8 and molecular alignment of the compound



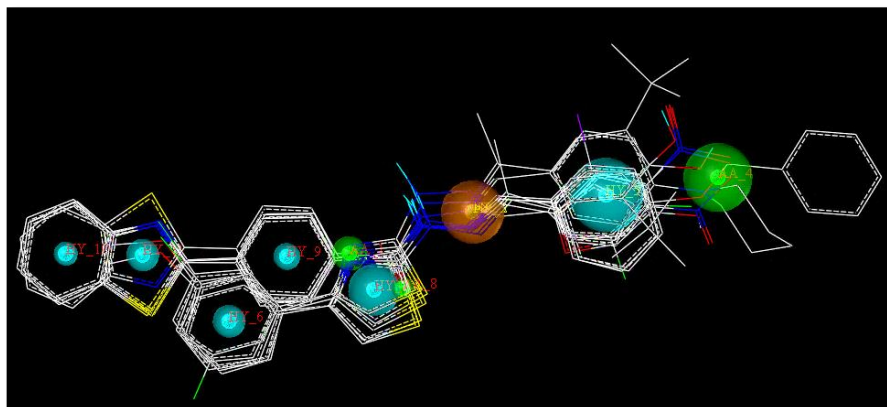


**Figure 7: Alignment of all test set compounds using pharmacophore modelling.**

**Table 2: The parameter values of Training set for each pharmacophore model:**

NAME	Specific.	N_HITS	FEATS	PARETO	Energy	Steric	HBOND	MOL_QRY
Model_001	3.818	-16	8	0	12.16	1344.7	328.5	102.39
Model_002	3.651	-16	9	0	11.05	1302.6	326.7	101.73
Model_003	3.812	-16	8	0	15.43	1431.7	326.1	103.38
Model_004	1.66	-16	9	0	8.05	1217.9	321.6	104.1
Model_005	3.823	-16	8	0	10.95	1338.4	320.8	104.34
Model_006	4.979	-16	8	0	17.59	1255.7	336	107.9
Model_007	3.814	-16	8	0	15.09	1308.6	325	107.49
Model_008	3.822	-16	8	0	10.95	1292.2	326.7	72.97
Model_009	3.8	-16	9	0	9.89	1340.7	322.1	66.9
Model_010	3.825	-16	8	0	8.36	1159.2	326.5	88.92

Contributions of steric and electrostatic fields were 0.507 and 0.493, respectively. The actual and predicted  $pIC_{50}$  values of the training and test set by

the model 7 (MMFF94 charge) [17-18] are listed in table. The graph of actual versus predicted  $pIC_{50}$  of the training and test set of model 29.

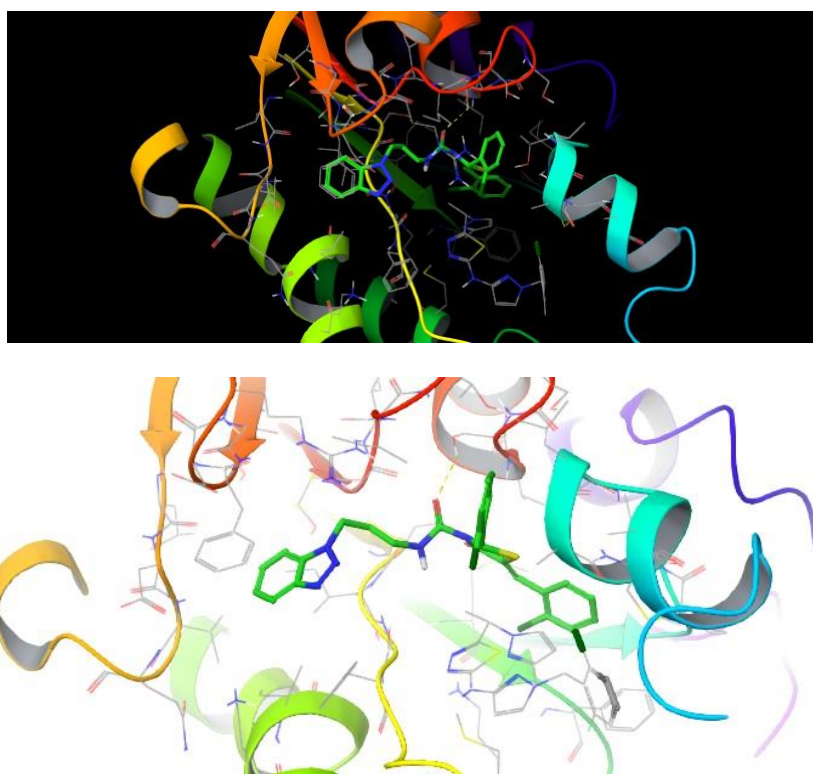
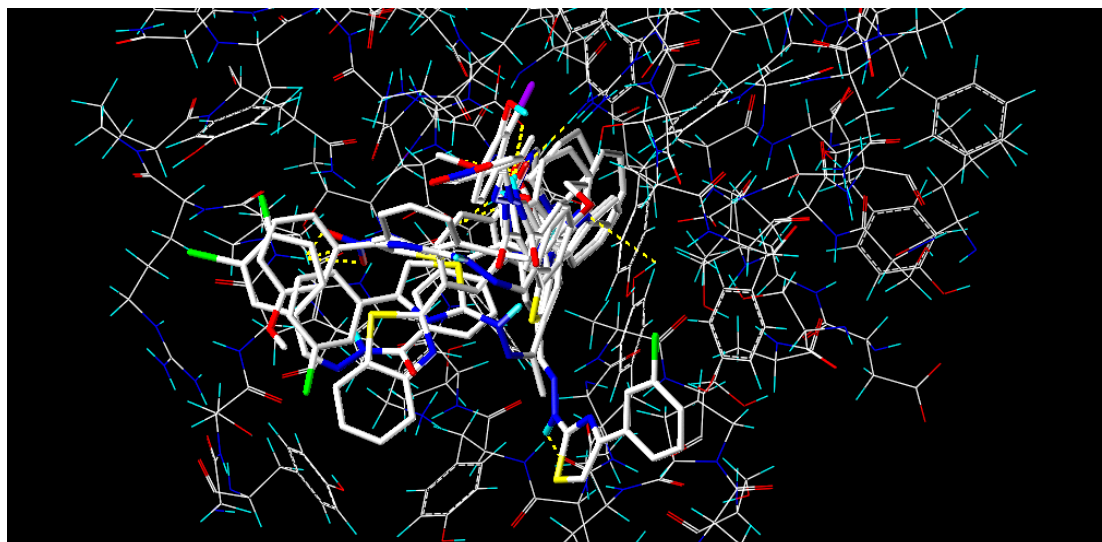


**Figure 8: Full Docking view of all compounds on 5JFO PDB**



Training Compound:

Test Compound:

**CONCLUSION:**

The explored CoMFA and CoMSIA models provided information about favorable and unfavorable region while HQSAR provides information about positive, negative and intermediate contribution of sub-structural fingerprint requirements for imparting the biological activity. The CoMFA, CoMSIA and HQSAR contour maps revealed sufficient information to understand the structure-activity relationship (SAR) and to recognize structural features influencing inhibitory activity. Based on the SAR study generated by molecular modelling analysis, one hundred and two novel oxidoreductase inhibitor derivatives were successfully designed exhibiting moderate predicted activities in all three applied computational approaches. The pharmacophore model developed helped us to obtain the common active pharmacophore regions along with the hydrophobe, donor and acceptor regions. All selected 2,3-imidazole and 2,4-imidazole analogues showed good alignment.

**REFERENCES:**

1. Abdullah A, Peeters A, Courten M, Stoelwinder J. The magnitude of association between overweight and obesity and the risk of diabetes: a meta-analysis of prospective cohort studies. *Diabetes research and clinical practice*. 89, 2010, 309–19.
2. Alberti K & Zimmet Z. Definition, diagnosis and classification of diabetes mellitus and its complications: Report of a WHO Consultation. *Diagnosis and classification of diabetes mellitus*. 1, 1999, 125.
3. Bethel M, Mark N, Feinglos M & Angelyn K. Type 2 diabetes mellitus: an evidence-based approach to practical management Totowa Humana Press. 2, 2008, 462.
4. Chandalia H. RSSDI textbook of diabetes mellitus Jaypee Brothers Medical Publishers New Delhi. 2, 2012, 235.
5. Christian P & Stewart C. Maternal micronutrient deficiency, fetal development, and the risk of chronic disease. *The Journal of nutrition*. 140, 2010, 437–45.
6. Cohen P & Goedert M. GSK3 inhibitors: development and therapeutic potential. *Nature Review of Drug Discovery*. 3, 2004, 479–48.
7. Cooke D & Plotnick L. Type 1 diabetes mellitus in pediatrics". *Paediatric Review*. 11, 2008 374–84.
8. Zhang S, Xu Z, Gao C, Ren QC, Chang L, Lv ZS, Feng LS. Triazole derivatives and their anti-tubercular activity. *European journal of medicinal chemistry*. 2017 Sep 29; 138:501-13.
9. H.S. Sutherland, A. Blaser, I. Kmentova, S.G. Franzblau, B. Wan, Y. Wang, Z. Ma, B.D. Palmer, W.A. Denny, A.M. Thompson, *J. Med. Chem.* 53 (2010) 855-866
10. J. Ramprasad, N. Nayak, U. Dalimba, P. Yogeewari, D. Sriram, *Bioorg. Med. Chem. Lett.* 25 (2015) 4169-4173.
11. K.D. Thomas, A.V. Adhikari, I.H. Chowdhury, E. Sumesh, N.K. Pal, *Eur. J. Med. Chem.* 46 (2011) 2503-2512.
12. K.K. Kumar, S.P. Seenivasan, V. Kumar, T.M. Das, *Carbohydr. Res.* 346 (2011) 2084-2090.
13. C. Menendez, A. Chollet, F. Rodriguez, C. Inard, M.R. Pasca, C. Lherbet, M. Baltas, *Eur. J. Med. Chem.* 52 (2012) 275-283.
14. S.R. Patpi, L. Pulipati, P. Yogeewari, D. Sriram, N. Jain, B. Sridhar, R. Murthy, A. Devi T, S.V. Kalivendi, S. Kantevari, *J. Med. Chem.* 55 (2012) 3911-3922.

- 15.K. Ozadali, O.U. Tan, P. Yogeeswari, S. Dharmarajan, A. Balkan, *Bioorg. Med.Chem. Lett.* 24 (2014) 1695-1697.
16. C.G. Bonde, A. Peepliwal, N.J. Gaikwad, *Arch. Pharm. Chem. Life Sci.* 343(2010) 228e236.
- 17.Z.Q. Li, Y.S. Liu, X.G. Bai, Q. Deng, J.X. Wang, G.N. Zhang, C.L. Xiao, Y.N. Mei, Y.C. Wang, *RSC Adv.* 5 (2015) 97089-97101.
- 18.Z. Li, X. Bai, Q. Deng, G. Zhang, L. Zhou, Y. Liu, J. Wang, Y. Wang, *Bioorg. Med.Chem.* 25 (2017) 213-220.